Brain Effective Connectivity Analysis Facilitates the Treatment Outcome Expectation of Sound Therapy in Patients With Tinnitus

Han Lv, Jinduo Liu, *Member, IEEE*, Qian Chen, Zuozhen Zhang, Zhaodi Wang, Shusheng Gong, Junzhong Ji, and Zhenchang Wang

***Abstract*— Tinnitus is associated with abnormal functional connectivity of multiple regions of the brain. However, previous analytic methods have disregarded information on the direction of functional connectivity, leading to only a moderate efficacy of pretreatment planning. We hypothesized that the pattern of directional functional connectivity can provide key information on treatment outcomes. Sixty-four participants were enrolled in this study: eighteen patients with tinnitus were categorized into the effective group, twenty-two patients into the ineffective group, and twenty-four healthy participants into the healthy control group. We acquired resting-state functional magnetic resonance images prior to sound therapy and constructed an effective connectivity network of the three groups using an artificial bee colony algorithm and transfer entropy. The key feature of patients with tinnitus was the significantly increased signal output of the sensory network, including the auditory, visual, and somatosensory networks, and parts of the motor network. This provided critical insights into the gain theory of tinnitus development. The altered pattern of functional information orchestration, represented by a higher degree of hypervigilance-driven attention and enhanced multisensory integration, may explain poor clinical outcomes. The activated gating function of the thalamus is one of the key factors for a good prognosis in tinnitus treatment. We developed a novel method for analyzing effective connectivity, facilitating an understanding of the tinnitus mechanism and treatment outcome expectation based on the direction of information flow.**

***Index Terms*— Tinnitus, sound therapy, fMRI, brain network, effective connectivity.**

Manuscript received 25 June 2022; revised 2 January 2023; accepted 31 January 2023. Date of publication 3 February 2023; date of current version 8 February 2023. The work of Han Lv was supported by the National Natural Science Foundation of China under Grant 62171297. The work of Jinduo Liu was supported by the National Natural Science Foundation of China under Grant 62106009. The work of Junzhong Ji was supported by the National Natural Science Foundation of China under Grant 62276010. The work of Zhenchang Wang was supported by the National Natural Science Foundation of China Grant 61931013. *(Han Lv and Jinduo Liu are co-first authors.) (Corresponding authors: Zhenchang Wang; Junzhong Ji.)*

This work involved human subjects or animals in its research. Approval of all ethical and experimental procedures and protocols was granted by the Ethics Committee of Beijing Friendship Hospital, Capital Medical University, under Application No. 2018-P2-182-01.

Han Lv, Qian Chen, and Zhenchang Wang are with the Department of Radiology, Beijing Friendship Hospital, Capital Medical University, Beijing 100050, China (e-mail: chrislvhan@126.com; cjr.wzhch@vip.163.com).

Jinduo Liu, Zuozhen Zhang, and Junzhong Ji are with the Beijing Municipal Key Laboratory of Multimedia and Intelligent Software Technology, College of Computer, Science and Technology, Faculty of Information Technology, Beijing University of Technology, Beijing 100124, China (e-mail: jjz01@bjut.edu.cn).

Zhaodi Wang and Shusheng Gong are with the Department of Otolaryngology Head and Neck Surgery, Beijing Friendship Hospital, Capital Medical University, Beijing 100050, China.

Digital Object Identifier 10.1109/TNSRE.2023.3241941

I. Introduction

FOR the estimated 10 to 25% of people with tinnitus worldwide [1], especially for the impeding cases that account for up to 7% of all patients with tinnitus [2], the sound of silence is a dream out of reach. Tinnitus can be alleviated using treatment methods recommended by the guideline [3]. One such option is sound therapy, which can achieve a modest outcome in most patients with tinnitus [4]. Unfortunately, approximately 20% to 40% of patients responded poorly to sound therapy [5].

Pretreatment planning for patients seeking sound therapy requires clinical, audiometry, questionnaire, and brain imaging assessments. However, the prognostic factors are controversial. A greater likelihood of better outcomes may be associated with several factors, including a short disease duration [4], the application of hearing aids or implants [4], a younger age [5], less skepticism [5], and a longer treatment duration [6]. Despite these findings, most of these factors cannot be applied to tinnitus treatment outcome expectation.

Currently, scientists agree that tinnitus is characterized by an altered brain network involving both the auditory and non-auditory brain regions. Pretreatment imaging features of resting-state functional networks can objectively reveal heterogeneity in the functional hierarchical organization of the brain. Various resting-state functional magnetic resonance imaging (fMRI) methods have been used to demonstrate the heterogeneity of the brain networks that are involved in patients with tinnitus [7], [8]. Several features of functional connectivity are being regarded as potential indicators of treatment prognosis [9], [10], [11], [12]. However, their predictive efficacy remains moderate. Previous functional connectivity analyses have evaluated the bidirectional correlation of the degree of synchrony of the blood-oxygen-level-dependent time series between brain regions [13]. A key obstacle is the lack of understanding of the direction of functional connectivity. As a result, the connection patterns are simplified, and a large amount of information is lost during analysis. Therefore, the mechanism of tinnitus remains unclear.

Recently, the Bayesian network (BN) method has been used for constructing brain effective connectivity (EC) because it can accurately infer connections between the brain regions [14]. In 2016 and 2019, Ji et al. developed two swarm intelligent algorithms (artificial immune and ant colony algorithms) to infer EC from fMRI data [15], [16]. Using two random global searching mechanisms in the candidate solution space, both methods obtained higher accuracy in identifying the directions of EC than traditional methods. However, owing to the equivalence class problem in a BN, the orientation of the connections could not be determined in some cases.

EC construction based on transfer entropy (TE) of the brain network is a new horizon for capturing the pattern of functional connectivity by analyzing global information flow [17]. This innovative method can elucidate pattern recognition of brain functional connectivity and the orientation of the connections. In this study, we employed an artificial bee colony (ABC) and TE to construct brain effective connectivity networks; the ABC algorithm has a strong global searching ability to obtain the optimal BN structure, and TE is useful to determine the orientation of the connections when two directions have the same score in a BN structure.

To validate the effectiveness of the proposed method, we conducted experiments using the Smith simulation dataset. Subsequently, we constructed EC networks from three participant groups: the effective group (EG; participants with tinnitus whose treatment are effective), ineffective group (IG; participants with tinnitus whose treatment are ineffective), and healthy control group (HCG; healthy participants). On the basis of the methodological innovation, we hypothesized that the pattern of pretreatment directional functional connectivity (effective connectivity) would provide key information on the treatment outcome. This study demonstrates a novel method to analyze resting-state fMRI so as to further our understanding of the mechanism of tinnitus.

II. Materials

This study was approved by the ethics committee of Beijing Friendship Hospital, Capital Medical University (ID. 2018-P2-182-01). The study was registered at ClinicalTrials.gov (ID. NCT03764826). Written informed consent was obtained from all the study participants.

A. Participants

Forty patients with non-pulsatile, tonal-like tinnitus and twenty-four healthy controls were prospectively enrolled in this study. All the participants were aged between 20 and 60 years and were right-handed. Any participant with pulsatile tinnitus, hyperacusis, head trauma, suspected Meniere's disease, dizziness, hyperacusis, other neurological diseases, or focal brain lesions were excluded.

B. Sound Therapy and Evaluation of Treatment Effects

For patients with tinnitus, we performed narrow-band sound therapy (20 min/session; three sessions/day; 24 weeks) using the SpeechEasy eMasker® (Micro-DSP Technology Co., Ltd., China). The sound was determined by clinicians with more than 10 years of tinnitus treatment experience in our institution's department of otolaryngology. We examined the tinnitus frequency (Tf), minimum masking levels, tinnitus pitch matching, and loudness matching (L). The loudness of the sound was set to L-5 dB. The bandwidth was set according to the Tf at 1/3 octave. The sound was delivered through headphones. The HCG did not receive any treatment.

For patients with tinnitus, we acquired the Tinnitus Handicap Inventory (THI) score. The THI is a self-reported measure that is commonly used to evaluate the severity of tinnitus. In accordance with previous studies, the treatment was defined as effective when the THI score reduced by 17 points or more or reduced to 16 points [18]. To guarantee consistency between the scores and imaging results, the THI scores were acquired on the same day prior to medical imaging data acquisition and treatment as well as on the same day of treatment completion.

C. Medical Imaging Data Acquisition

We performed high spatial T1-weighted imaging and blood-oxygenation-level-dependent resting-state fMRI on patients and healthy controls at the time of admission. Patients were also scanned 24^{th} weeks after treatment. For all the participants, data were obtained using a 3.0T MRI system (Prisma; Siemens, Erlangen, Germany) with a 64-channel phase-array head coil. The scanning parameters of fMRI were as follows: total volumes = 240; 33 slices; slice thickness/gap = 3.5 mm/1 mm; repetition time/echo time = 2,000 ms/30 ms; matrix = 64 s × 64; and field of view = 224 × 224 mm^2.

III. Methods

A. Data Preprocessing

We applied the Graph-theoretical Network Analysis Toolkit (http://www.nitrc.org/projects/gretna/) [19] that was installed in MATLAB 2016a (Math Works, Natick, MA) for preprocessing fMRI data of all the participants. In brief, the first 20 volumes of fMRI data were discarded. Slice timing, realignment, spatial normalization into the Montreal Neurological Institute template using T1-weighted imaging, resampling to 3 mm × 3 mm × 3 mm voxels, smoothing using a 6-mm full width at half-maximum Gaussian kernel, and detrend temporal filtering (between 0.01 and 0.1 Hz) were performed accordingly. Subsequently, we extracted the time-series data of each region of interest (ROI) according to a brain atlas that included 246 sub-brain regions based on connectional architecture [20].

We employed the ABC algorithm and TE to construct a brain EC network from the fMRI time-series data, named ABCTE. Let X_i be a brain region variable and let the bold letter $\mathbf{X}_i^T = (x_i^1, x_i^2, \ldots, x_i^t, \ldots, x_i^T)$ $(t = 1, 2, \ldots, T)$ denote the time series of the brain region X_i (the number of data points is T), where x_i^t denotes the value of the fMRI time series of region X_i at time t. The brain EC network is a directed graph $\mathcal{G} =< \mathbf{V}, \mathbf{E} >$, where $\mathbf{V}$ is a group of nodes (brain regions), and each node $X_i \in \mathbf{V}$ denotes a brain region or ROI; $\mathbf{E}$ is a group of arcs, and each arc $X_i \rightarrow X_j \in \mathbf{E}$ characterizes a causal effect (EC), wherein one brain region X_i impacts the other X_j. That is, the node X_i is the parent node of the node X_j. Therefore, approaches to EC network construction typically concentrated on identifying a directed graph model $\mathcal{G}$ that fits a set of fMRI data $\mathcal{D}$ according to a scoring criterion $S(\mathcal{G}|\mathcal{D})$.

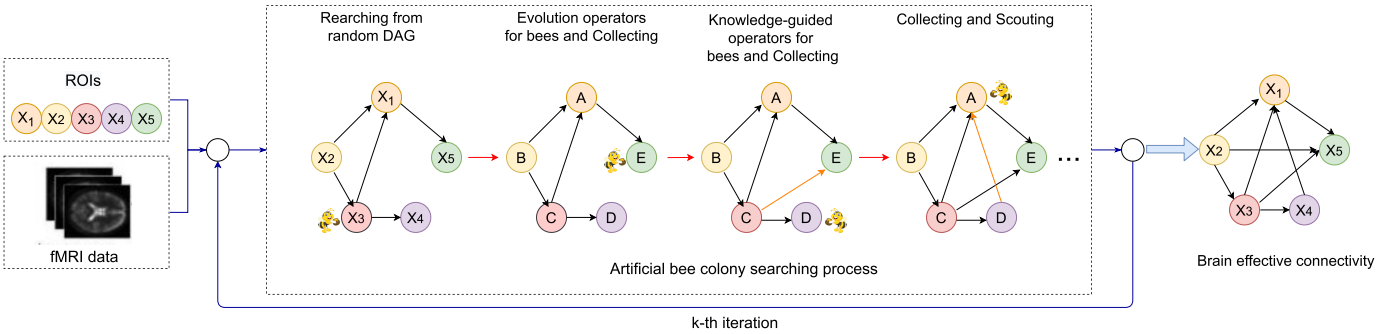

Fig. 1. The schematic diagram of ABC.

B. EC Network Construction

In this section, we employed the ABC algorithm to search for an optimal EC network structure with the best $K2$ metric. The ABC algorithm is a global optimization method based on the meta-heuristic mechanism, which has a high convergence velocity but is difficult to apply in local optimization.

Fig. 1 shows a flowchart of the ABCTE algorithm. First, we obtained random directed acyclic graphs (DAGs) from the brain regions using the fMRI data. Subsequently, we performed the search process of the ABC algorithm repeatedly until we obtained the brain EC network with the highest score. The search phase for the brain EC network consisted of three major steps. The first two steps involved bringing the worker bees and onlooker bees to the food sources who would perform a partial search for neighbor solutions. Workers and onlookers used different methods to search for the neighbor solutions. Workers applied four fundamental evolution operators (insert, deletion, reverse, and move) to obtain a new neighbor solution that was close to the current solution, and onlookers performed two knowledge-driven operators or four evolution operators using a random selection rule. The third step used scout bees as explorers to search for new food sources for each food source that had been completely depleted. Each scout had no guidance while searching for new food sources, which means that a scout can find any type of food source to overcome the stagnation phenomenon of solutions. The collection processes were performed collectively in this algorithm.

In the ABC, each bee k started with an empty graph G_0 and progressively constructed the connected solution by adding one arc at a time until the solution obtained the highest score. The specific process of searching for EC is described as follows: The probabilistic transition rule of a bee k for choosing a directed edge from the current candidate edges at runtime t is defined as

$$i, j = \begin{cases} arg\max_{r,l\in DA_k}\{[\tau_{rl}(t)]\cdot[\eta_{rl}(t)]^{\beta}\}, & \text{if } q \le q_0 \\ I, J, & \text{otherwise} \end{cases} \quad (1)$$

where $\tau_{rl}(t)$ and $\eta_{rl}(t)$ respectively denote the pheromone intensity information and the heuristic information of the arcs (EC); β is a parameter that controls $\eta_{rl}(t)$ to effect selecting candidate arcs; $DA_k(r, l \in DA_k)$ denotes a group of all alternative arcs which satisfies DAG constraint conditions and whose heuristic information is greater than zero; $_0$ $(0 \le_0 < 1)$ is a parameter that determines the bee to exploit or explore, where exploitation means selecting arcs by pheromone intensity and heuristic information, and exploration means global random selecting arcs; q is a parameter which obeys the standard normal distribution; I, J denotes two nodes which are selected according to the following rule of possibility:

$$p_{ij}^{k}(t) = \begin{cases} \dfrac{[\tau_{ij}(t)]^{\alpha}\cdot[\eta_{ij}(t)]^{\beta}}{\sum_{r,l\in DA_k}[\tau_{rl}(t)]^{\alpha}\cdot[\eta_{rl}(t)]^{\beta}}, & \text{if } i, j \in DA_k \\ 0 & \text{otherwise} \end{cases} \quad (2)$$

where parameter α denotes the concentration of the pheromone information $\tau_{rl}(t)$ left by the bees. For the purpose of obtaining the optimal structure which has the maximal scoring metric, the heuristic function of a directed arc is defined as follows:

$$\eta_{ij}(t) = f(X_i, PA(X_i)\cup X_j) - f(X_i, PA(X_i)). \quad (3)$$

Let G^+ denote the optimal structure found at present and $f(G^+ : D)$ is representing the metric score of G^+. At the end of each iteration $\tau_{ij}(t)$ are updated to conserve the information of the best solution which is found in the previous iterations. The global updating rule is

$$\begin{aligned} \tau_{ij}(t) &= (1-\rho)\tau_{ij}(t-1) + \rho \triangle \tau_{ij}(t) \\ \triangle\tau_{ij}(t) &= \begin{cases} \dfrac{1}{|f(G^+ : D)|}, & if\ a_{ij} \in G^+ \\ \tau_{ij}(t-1), & otherwise, \end{cases} \end{aligned} \quad (4)$$

where $0 < \rho \le 1$ is also a parameter of the pheromone evaporation.

When searching for neighbor solutions, we present four fundamental operators and two knowledge-driven operators for workers (bee) and onlookers (bee) to search for the neighbors' solutions. As for workers, they apply four fundamental operators to search for a new solution G_h (h is the number of arcs). These four operators can be described as:

- *Insert* The operator first randomly selects two nodes X_j and X_i where $i \neq j$, and $X_i \in X \setminus PA(X_j)$. Then, add an arc $a_i j = X_i \to X_j$ to $G_{h+1} = G_h \cup \{a_{ij}\}$ if G_{h+1} still a directed acylic graph.
- *Delete* The operator first randomly selects an arc a_{ij} from nodes X_i to X_j which is present in the G_h, then deletes it from G_h. Namely, a new solution $G_(h-1) = G_h \setminus \{a_{ij}\}$ is abtained.
- *Reverse* The operator randomly selects an arc a_{ij} from G_h, and alters the direction of the arc if the reversion of the arc still forms a DAG. Then a new solution, $G_h \setminus \{a_{ij}\} \cup \{a_{ij}\}$, is obtained.
- *Move* The operator respectively selects a parent node of two nodes X_i and X_j whose parent sets are not empty, denotes $X_k \in PA(X_i)$ and $X_l \in PA(X_j)(k \neq l)$, then changes X_k with X_l if $X_l \in (X \setminus (PA(X_i) \cup \{X_i\}))$,

$X_k \in (X \setminus (PA(X_j) \cup \{X_j\}))$ and still forms a DAG. Namely, this operator simultaneity alters the parent sets of two nodes.

Unlike workers, onlookers employ these four fundamental operators or two knowledge-driven operators according to a random selection rule. The knowledge-driven operators are specifically developed for onlookers based on the $K2$ scoring metric. These operators first take the $K2$ metric of all possible arcs into consideration and then select which arc to remove or insert. Note that the $K2$ metric of each possible arc X_{ij} is computed and stored before the learning algorithm is executed. These two knowledge-driven operators can be described as:

- $knowledge-driveninsertoperator$ The operator is an extended version of the insert operator that is mentioned above. When this operator determines to add an arc to the current solution G_h, it examines the stored $K2$ metric of the arcs not in G_h, then the arcs with a higher $K2$ metric will have higher probabilities to be added. The $K2$ metric of a network structure can be decomposed into that of each individual variable, and the objective of our algorithm is to find a network structure with the maximal $K2$ metric. If we want to insert an arc from some node to X_i, it is better to select an arc with a higher $K2$ metric, because it is more likely to increase the $K2$ metric $f(X_i, PA(X_i))$ of node X_i.
- $knowledge-drivendeleteoperator$ The operator is an extended version of the delete operator mentioned above. When the operator decides to select an existing arc of the current solution G_h, the arcs with a lower $K2$ metric are more likely to be deleted, which can minimize the decrement of the k2 metric of node X_j as far as possible.

Finally, the algorithm gets the current optimal solution G^+ when the iterations of ABC are ended or there is no way to make the score of the new solution higher by adding an arc. In detail, the algorithm obtains the same optimal solution for 5 successive generations, the search phase will end.

C. Directed Transfer Entropy Estimation

Suppose that we have a fMRI time series data set $\mathcal{D} = (\mathbf{X}_1, \ldots, \mathbf{X}_N) \in \mathbb{R}^{T\times N}$, where N is the number of variables (brain regions) and T is the number of time points (all variables have the same length). Then the data $\mathcal{D}$ with n brain regions can be represented as:

$$\begin{aligned}\mathcal{D} &= \mathbf{X}_1, \mathbf{X}_2, \ldots, \mathbf{X}_N \\ &= (\mathbf{X}_1, \mathbf{X}_2, \ldots, \mathbf{X}_N)^\top \in \mathbb{R}^{T\times N}.\end{aligned} \tag{5}$$

For a brain region X, the differential entropy $H(X)$ is defined as

$$H(X) = -\int_{\mathbb{R}^d} f(x)\log f(x)dx, \tag{6}$$

where $f(x)$ is the probability density function of X on $\mathbb{R}^d$, "log" always means natural logarithm so that information is measured in natural units. Assume $f(x)$ is differentiable, then $H(X)$ can be estimated by the Kozachenko-Leonenko (KL) differential entropy estimator, which is a kind of non-parametric estimator method based on k-nearest neighbor

TABLE I
DESCRIPTION OF THE 5 SIMULATIONS [14]

Sim	Nodes	Session (s)	TR (s)	Noise (%)	HRF (s)	Subjects
1	5	600	3.00	1.0	0.5	50
2	10	600	3.00	1.0	0.5	50
3	15	600	3.00	1.0	0.5	50
4	50	600	3.00	1.0	0.5	50
5	5	600	0.25	0.1	0.0	50

entropy estimators. Then we can obtain

$$H(X) = -\psi(k) + \psi(l) + \log(1) + \frac{1}{l}\sum_{i=1}^{l}\log\epsilon(i). \tag{7}$$

Let us consider the joint random variable (X_i, X_j) with the maximum norm, then we replace d_a with $d_a + d_b$, V_{da} with $V_{da}V_{db}$, and we can estimate $H(X_i, X_j)$ by

$$\begin{aligned}H(X_i, X_j) &= -\psi(k) + \psi(l) + \log(V_{da}V_{db}) \\ &\quad + \frac{d_a + d_b}{l}\sum_{i=1}^{l}\log\epsilon(i) \\ &= -\psi(k) + \psi(l) + \log(1) + \frac{2}{l}\sum_{i=1}^{l}\log\epsilon(i).\end{aligned} \tag{8}$$

More specifically, the transfer entropy from bran region X_j to another region X_i can be written as

$$T_{X_j\to X_i} = H(X_i|X_i^m) - H(X_i|X_i^m, X_j^n), \tag{9}$$

where X_i^m is the m-lag history of X_i, and X_j^n is the n-lag history of X_j, $T_{X_j\to X_i}$ measures the amount of directed information flow from X_j to X_i. Next, we decompose TE into a sum of four individual entropies:

$$\begin{aligned}T_{X_j\to X_i} &= H(X_i, X_i^m) + H(X_i^m, X_j^n) \\ &\quad - H(X_i, X_i^m, X_j^n) - H(X_i^m),\end{aligned} \tag{10}$$

where each entropy can be estimated by Eqs. 7 and Eqs. 8.

D. Algorithm Description

To clearly illustrate the process of our method, we have provided a pseudocode of the proposed method. The algorithm proposed in this paper is summarized in Algorithm 1. The process of the ABCTE algorithm can be divided into three phases: 1) initialization, 2) search for an EC network, and 3) selecting and returning the best EC network.

The ABCTE algorithm began with an initial group of DAGs produced by the initialization function (ConstructGraph()). Each DAG represents a solution (food source) and is evaluated using the $K2$ metric. In the search for an EC network phase, the search was carried out with the neighbor search phases of the workers, onlookers, and scouts. For each iteration, every worker was first connected with a solution; then, it employed $Neighbor\_search()$ function (insert, deletion, reverse, move) to find a new solution that was adjacent to the associated solution. In the search operator stage, the workers moved to a new solution or continued to stay where they were depending on whether the $k2$ metric of this new solution was better than the $k2$ metric of the current solution. After the search

Algorithm 1 Effective Connectivity Network Construction by ABC and Transfer Entropy (ABCTE)

Input: fMRI dataset.
Output: Brain effective connectivity network.
Initialization:
Set parameters K, N, α, β, q_0, ρ, q_d, L;// $\tau_{ij}(0) = 1/n \cdot \mid \sum_{i=1}^{n} f(X(i), X_{pa}(i)) \mid$;
for $k = 1$ *to* K **do**
  $G_k(0)$=ConstructGraph();
end
repeat
  Neighbor search phases of workers.
  for $k = 1$ *to* K **do**
    Associate a worker with a $G_k(t)$;
    Evaluate $G_k(t)$;
    $G'_k(t)$= Neighbor_search $(G_k(t))$;
    $G_k(t)$ = argmax $\{f(G_k), f(G'_k)\}$;
  end
  Neighbor search phases of onlookers.
  for $l = 1$ *to* K **do**
    Select a solution;
    if $(q \leqslant q_d)$ **then**
      $G'_l(t)$= Neighbor_KG_search $(G_l(t))$;
    else
      $G'_l(t)$= Neighbor_search $(G_l(t))$;
      $G_l(t)$ = argmax $\{f(G_l), f(G'_l)\}$;
    end
  end
  Exploring new solutions by scouts.
  for $k = 1$ *to* K **do**
    Moving the worker to satisfied solution by integrating onlookers'search ;
    if $G_k(t) = G_k(t-1)$ **then**
      $C_k = C_k + 1$;
    else
      $C_k = 0$;
    end
    if $C_k = L$ **then**
      Abandon solution $G_K(t)$ and the associated worker k becomes a scout ;
      $G_k(t)$ = ConstructGraph() and again become an worker;
    end
  end
  Memorize the best solution $G_k(t)$ found so far;
  Perform global pheromone update;
until $t = 0$ *is equal or greater than* N;
if $G_k(i)$ *and* $G_k(j)$ *with the same score* **then**
  Select the graph whose arc with higher TE;
  $G^+ = max(G_k(i), G_k(j))$.
end
Return: Brain effective connectivity network G^+ with the highest score.

phase, these workers shared information about their solutions with the onlookers. The onlookers selected the preferred solutions, performed two knowledge-driven operators or four fundamental search operators, determined a new solution adjacent to the selected solution, and computed the k2 metric of the new solution. The worker was brought to the best solution by comparing all the k2 metrics of these solutions. If the k2 metric of the solution connected with the worker does not improve after a preset number of iterations (limit), then this solution was trapped in the local optimum; here, the worker abandoned the solution and became a scout. According to the pheromone information left on arcs and heuristic information, this scout could reconstruct a new solution (food source) and become a worker again. Once all scout solutions were determined, the next iteration of the ABCTE algorithm began. This iteration was repeated until the termination conditions were satisfied. Finally, the ABCTE provided the solutions with the best k2 value in all iterations. If the solutions had the same score, we selected the better solution with arcs that had a higher TE as the learned EC network.

IV. Results

A. Data Description

1) Benchmark Simulated Data: We employed benchmark simulated data with a ground truth network to test the performance of the proposed method. The simulated data were generated by Smith et al. [14] and are widely used for evaluating the performance of methods for inferring EC. Current research shows that the number of nodes is the main factor affecting the performance of learning methods; thus, we chose four simulation datasets, each with a different numbers of nodes. Besides, to demonstrate the factor of low TR and HRF variability for different methods, we employed the simulation with neural lag = 100 ms. The descriptions of the five simulations are shown in Table I.

2) Data of Patients With Tinnitus: Eighteen patients were effectively treated with sound therapy (EG), whereas 22 patients were non-responsive to the treatment (IG), according to the THI scores at the 24^{th} week. The clinical factors between the EG, IG, and HCG (Table II) were not significantly different. Additionally, the changes in THI scores and percent improvement in THI scores were significantly different between the EG and IG (see Table II).

B. Experiments on Simulated Data

To demonstrate the competitiveness of the ABCTE algorithm, we compared it with seven other methods: the prediction correlation (P-corr) method [21], linear non-Gaussian acyclic model (LiNGAM) [22], Granger causality (GC) method [23], [24], generalized synchronization (GS) method [25], Patel's condition dependence measurement method (Patel) [26], AIAEC [15], and VACOEC [16]. In this experiment, we employed the F1 value to evaluate the performances of the different methods. The results are shown in Table III.

As shown in Table III, the number of nodes in the Sim1-4 data sets increased from 5 to 10, 15, and 50. We found that the number of brain regions had an impact on the quality of the methods. By comparing the performances of the different methods sequentially using the Sim1-4 data sets, we observed that the majority of methods had a small $F1$ decrease. Compared with AIAEC and VACOEC, ABCTE had a better and more stable performance. In particular, when the node size of

TABLE II
PATIENT CHARACTERISTICS

	Tinnitus patients, Effective Group		Tinnitus patients, Ineffective Group		Healthy controls	*P-value*
	Baseline, n=18	Treated, n=18	Baseline, n=22	Treated, n=22	n=24	
Age (years)	51.8 ± 8.7		48.1 ± 9.6		$34-57(47.2 \pm 7.2)$	0.20^a
Gender (male/female)	8/10		11/11		10/14	0.85^b
Handedness	18 right-handed		22 right-handed		24 right-handed	$>0.99^a$
THI score	59.0 ± 23.3	17.1 ± 7.4	47.1 ± 26.4	50.8 ± 23.3	NA	$<0.01^c$
Δ THI score	41.9 ± 19.6		-3.6 ± 8.0		NA	NA
% improvement of THI score	69.5 ± 10.7		-13.9 ± 27.1		NA	NA
Duration, months	$\geq 6\& \leq 48$		$\geq 6\& \leq 48$		NA	NA
Tinnitus Pitch	$250-8,000$ Hz		$1,000-8,000$ Hz		NA	NA
Laterality	5 left, 2 right and 11 bilateral		4 left, 2 right and 16 bilateral		NA	0.73^b

TABLE III
THE *F*1 VALUE OF 8 ALGORITHMS ON 5 SIMULATIONS

Sim	Algorithms							
	P-corr	LiNGAM	GC	*GS*	*Patel*	AIAEC	VACOEC	ABCTE
Sim1	0.80	0.91	1.00	0.60	0.80	1.00	1.00	1.00
Sim2	0.75	0.87	0.64	0.82	0.82	0.91	0.92	0.92
Sim3	0.56	0.84	0.65	0.89	0.84	0.84	0.87	0.89
Sim4	0.56	0.68	0.58	0.79	0.77	0.75	0.82	0.84
Sim5	0.80	1.00	0.71	1.00	0.80	1.00	1.00	1.00

the data increased to 50, the $F1$ value of ABCTE reached 0.84, indicating better performance than those of the other seven methods. Thus, an increase in the number of nodes has an impact on the performance of the other algorithms, but ABCTE can still achieve a good and stable performance. From Sim5, we found that the temporal resolution and noise of the data may have constrained the lag-based methods (e.g., GC); however, they had no great impact on the identification performance of the BN methods.

C. Experiments on Data of Patients With Tinnitus

We applied the method to patients with tinnitus who enrolled in this study. The ROIs of the human brainnetome atlas applied in this study, as shown in Table IV, were grouped on the basis of the connectional architecture, including anatomical and functional connectivity information [20].

Fig.2 shows the learned brain EC networks of the three groups. The direction of the functional connectivity was successfully demonstrated for each ROI of the atlas. The column represented the information flow from the ROI to other brain regions. The row represented the information flow from the other brain regions to the ROI. The matrix value represented the strength of the EC between the brain regions.

As shown in Fig. 2, the HCG featured multiple groups of increased or decreased strength of EC. The grouped connectivity pattern was consistent with those of the groups of the brainnetome atlas. On analyzing patients with tinnitus, several forms of altered EC strength were significantly different among groups. As shown in Figs. 2 and 3, altered EC included a) the bilateral precentral gyrus as part of the motor network (ROI: 53 to 62), b) bilateral postcentral gyrus as part of the somatosensory network (ROI: 155 to 162), c) bilateral primary auditory cortex (ROI: 69 to 72), d) bilateral thalamus (ROI: 241 to 264), e) bilateral lateral occipital cortex (ROI: 199 to 208), and f) the bilateral medioventral occipital cortex (ROI: 189 to 198). These results validated the effectiveness of the computational method we demonstrated in this research based on real-world data.

TABLE IV
THE NUMBER AND CORRESPONDING REGIONS OF THE ANALYZED ROIS

ROI Number	Brain Regions
$1 \sim 14$	superior frontal gyrus
$15 \sim 28$	middle frontal gyrus
$29 \sim 40$	inferior frontal gyrus
$41 \sim 52$	orbital gyrus
$53 \sim 64$	precentral gyrus
$65 \sim 68$	paracentral lobule
$69 \sim 80$	superior temporal gyrus
$81 \sim 88$	middle temporal gyrus
$89 \sim 102$	inferior temporal gyrus
$103 \sim 108$	fusiform gyrus
$109 \sim 120$	parahippocampal gyrus
$121 \sim 124$	posterior superior temporal sulcus
$125 \sim 134$	superior parietal lobule
$135 \sim 146$	inferior parietal lobule
$147 \sim 154$	precuneus
$155 \sim 162$	postcentral gyrus
$163 \sim 174$	insular gyrus
$175 \sim 188$	cingulate gyrus
$189 \sim 198$	medioventral occipital cortex
$199 \sim 210$	lateral occipital cortex
$211 \sim 214$	amygdala
$215 \sim 218$	hippocampus
$219 \sim 230$	basal ganglia
$231 \sim 246$	thalamus

V. DISCUSSION

The main strength of our study is that we not only developed a new data-driven method to construct an EC network, but we also identified the direction of information flow of patients with tinnitus without a prior selection of ROIs in the functional connectivity analysis. The patterns of functional information orchestration for patients with tinnitus with different treatment outcomes were described more precisely than before, allowing us to better unveil the mechanisms of tinnitus.

The functional connectivity of brain networks in patients with tinnitus has always been controversial [27]. Pooled

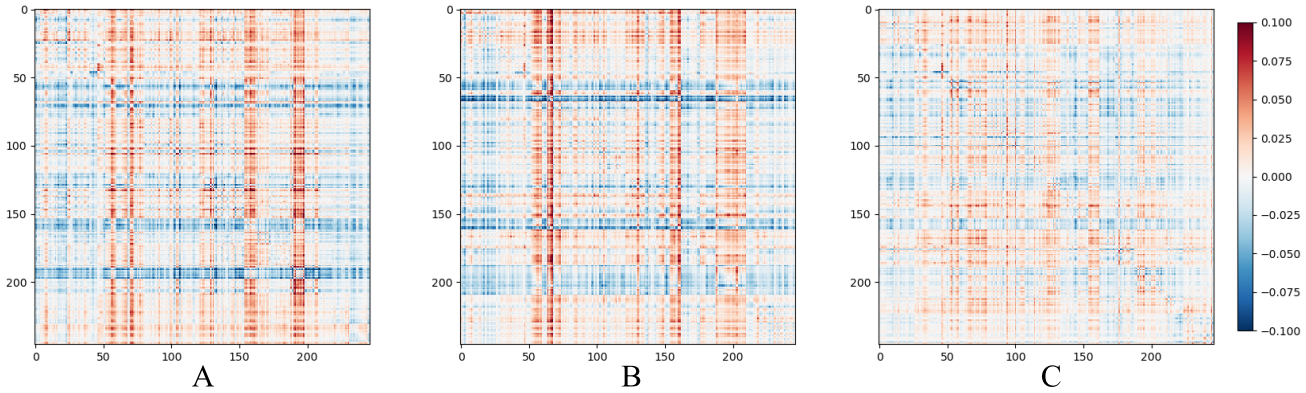

Fig. 2. The brain effective connectivity networks of the three groups. A, effective group. B, ineffective group. C, healthy controls.

imaging results may be of limited value in treatment outcome expectation irrespective of the direction of functional connectivity [9], [12], [28], [29]. Recently, several studies have focused on the directed functional connectivity in patients with tinnitus. However, limited results have been reported owing to the limitations of the applied research methods, leading to an incomplete understanding or misunderstanding of the information flow. This may have resulted from several brain regions being included in the investigation of the directional connectivity of patients with tinnitus [30], [31], [32]. Limited by the analytic method, researchers define the brain network they focused on prior to data analysis, which may have led to subjective bias in their research. In addition, the applicability and appropriateness of the widely used Granger causality analysis in neuroscience studies is of concern [33].

To address this problem, we employed TE, which can capture temporal information from fMRI time series, to measure the causal relationships among brain regions. In addition, we employed the ABC algorithm, which adopts a stochastic search mechanism, whose quality is usually higher than that of solutions obtained by traditional searching methods. In addition, the ABC algorithm can easily support information fusion because it can integrate useful information in the searching process. Thus, the pattern of functional information orchestration in the whole brain of the participants was precisely described using our method. The results can be applied as a neural signature for the analyzed participants, especially for patients with tinnitus with different outcomes. In addition, this method is characterized by optimal appropriateness. The innovated analytic method provides a novel approach to explore the brain network. It can also be applied to other types of participants to analyze the EC of the brain network when only resting-state fMRI is performed.

In our study, multiple enhanced linkages among brain regions were identified, especially for multiple sensory networks (including auditory, visual, and somatosensory networks) and parts of motor networks. Our results support the hypothesis that tinnitus may lead to the reorganization of co-activity between auditory and other sensory networks [34]. However, decreased EC was detected in several brain regions, especially in the thalamus.

The mechanism of tinnitus has been widely discussed. The subcortical pathways, especially the thalamus, are key brain regions that may affect the development of tinnitus. According to the gating theory, an attenuation of signal transmission via the subcortical neural pathways external to the peripheral sensory pathways may be the mechanism that inhibit the presence of tinnitus. The thalamus suppresses tinnitus signal transmission and mediates the thalamocorticothalamic network to avoid the development of tinnitus [35], [36]. Decreased signal transmission in the bilateral thalamus has also been observed in patients with tinnitus after successful sound therapy [37], [38], [39]. In our study, the average strength of the EC of the thalamus (ROI: 231 to 246) in EG (-1.09×10^{-2}) was lower than those of IG (-0.51×10^{-2}) and HCG (0.3×10^{-3}), representing less information output in EG, e.g., increased activated gating function in EG. Thus, we proposed that the activated gating function of the thalamus was a key factor for good prognosis of tinnitus treatment, in line with the hypothesis that was previously made [40].

Patients with tinnitus with hearing loss may be associated with top-down as well as bottom-up modulation [7]. Previous studies have reported reduced signal transmission to the auditory cortex using electroencephalography data analysis [41]. However, studies have also reported that the primary auditory cortex and somatomotor networks are characterized by increased connectivity in patients with tinnitus [42], indicating possibly heavier information flow of the brain regions. Thus, the communication from auditory and somatomotor networks to other brain regions may be enhanced. Theoretically, tinnitus could conversely amplify the effect of auditory nerve activity via a top-down influence [43], [44], [45]. In our study, IG demonstrated significantly higher signal output of the primary auditory cortex than EG did. As a result, the function of the sensory network is not only to receive signals but also to transmit signals in patients with tinnitus.

The mechanism of gain may serve as the basis to explain the information flow in patients with tinnitus [40]. Gain refers to a change in the input–output function. A given output can be elicited by a weaker input. Thus, the direction of the information flow should be critically considered. For patients with tinnitus, both the auditory cortex and thalamus are the cores of gain models. The changes in information direction between brain regions may explain the different states of the patients. In this study, the increased signal output of the sensory network was observed in accordance with the decreased signal transmission of the thalamus. An increased amplitude of low-frequency oscillations was found in the

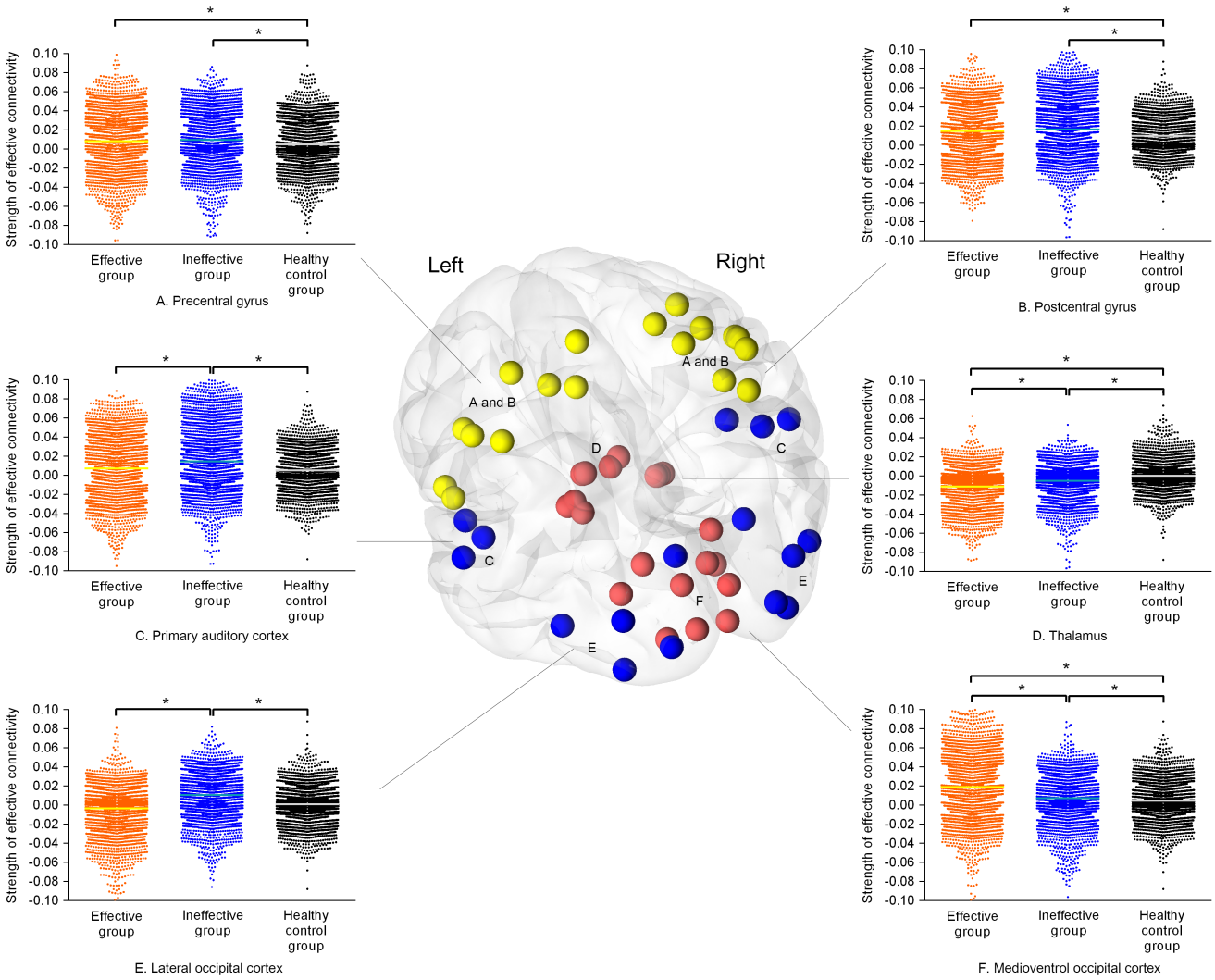

Fig. 3. There were several groups of altered strength of EC that significant different among groups. Yellow dots represent the strength of EC of the tinnitus patients were higher than that of HCG. Blue dots represent the strength of the EC were higher in IG than that of EG and HCG, which indicated poor prognosis. Red dots represent significant differences of the strength of EC among the three groups. EC, effective connectivity; EG, effective group; IG, ineffective group; HCG, healthy control group.

auditory cortex of patients with tinnitus, indicating a higher burst firing of neural activity [46]. After successful suppression of tinnitus, the low-frequency amplitude of the auditory cortex is also reduced [47]. In addition, the function of the thalamus as an underactive gain control mechanism may also be the reason for inducing positive feedback from the auditory cortex. Thus, in accordance with the concept of the gain theory, a given output from the auditory cortex may be elicited from weaker inputs from the thalamus.

A significant difference was observed in the occipital cortex between the EG and IG. As shown in Fig. 2, the IG featured a relatively lower strength of EC in the bilateral medioventral occipital cortex than the EG (ROI: 189 to 198) but a higher information outflow in the bilateral lateral occipital cortex and primary auditory cortex (ROI: 199 to 208 and 69 to 72, respectively). These may be key factors that influence treatment outcomes. The lower strength of connectivity of the medioventral occipital cortex is associated with hypervigilance-driven attention [48]. In addition, the lateral occipital cortex is a neural substrate for multisensory integration [49]. Features that are significantly different between the EG and HCG, e.g. a higher degree of hypervigilance-driven attention and enhanced multisensory integration, may be the reason for the failure of sound therapy in patients with tinnitus.

VI. Conclusion

Using an ABC and TE, we successfully constructed an EC network for the three groups of participants. We provided a novel approach for analyzing resting-state fMRI data and understanding the mechanism of tinnitus, indicating that the significant increase in signal output of the sensory network and parts of the motor network is a key feature of the gain theory for tinnitus acquisition. The deactivated brain EC of the medioventral occipital cortex and the enhanced EC of the lateral occipital cortex and primary auditory cortex may indicate a poor prognosis of sound therapy. The activated function of the thalamus is a key factor for good prognosis in tinnitus treatment. The mechanism of tinnitus can be better understood, and clinical outcomes can be expected prior to treatment by applying the proposed analytic method.

REFERENCES

[1] C. A. Bauer, "Tinnitus," *New England J. Med.*, vol. 378, no. 13, pp. 1224–1231, 2018.

[2] J. M. Bhatt, H. W. Lin, and N. Bhattacharyya, "Prevalence, severity, exposures, and treatment patterns of tinnitus in the United States," *J. Amer. Med. Assoc. Otolaryngol., Head Neck Surg.*, vol. 142, no. 10, pp. 959–965, 2016.

[3] D. E. Tunkel et al., "Clinical practice guideline: Tinnitus," *Otolaryngol., Head Neck Surg.*, vol. 151, no. 2, pp. S1–S40, 2014.

[4] M. Pienkowski, "Rationale and efficacy of sound therapies for tinnitus and hyperacusis," *Neuroscience*, vol. 407, pp. 120–134, May 2019.

[5] G. D. Searchfield, M. Durai, and T. Linford, "A state-of-the-art review: Personalization of tinnitus sound therapy," *Frontiers Psychol.*, vol. 8, p. 1599, Sep. 2017.

[6] J. Simoes et al., "Toward personalized tinnitus treatment: An exploratory study based on internet crowdsensing," *Frontiers Public Health*, vol. 7, p. 157, Jun. 2019.

[7] D. De Ridder et al., "An integrative model of auditory phantom perception: Tinnitus as a unified percept of interacting separable subnetworks," *Neurosci. Biobehav. Rev.*, vol. 44, pp. 16–32, Jul. 2014.

[8] F. T. Husain, "Neural networks of tinnitus in humans: Elucidating severity and habituation," *Hearing Res.*, vol. 334, pp. 37–48, Apr. 2016.

[9] J. J. Han, D. D. Ridder, S. Vanneste, Y.-C. Chen, J.-W. Koo, and J.-J. Song, "Pre-treatment ongoing cortical oscillatory activity predicts improvement of tinnitus after partial peripheral reafferentation with hearing aids," *Frontiers Neurosci.*, vol. 14, p. 410, May 2020.

[10] L. Han et al., "Baseline functional connectivity features of neural network nodes can predict improvement after sound therapy through adjusted narrow band noise in tinnitus patients," *Frontiers Neurosci.*, vol. 13, p. 614, Jul. 2019.

[11] S. H. Kim et al., "Neural substrates predicting short-term improvement of tinnitus loudness and distress after modified tinnitus retraining therapy," *Sci. Rep.*, vol. 6, no. 1, pp. 1–10, Jul. 2016.

[12] Q. Chen et al., "Pretreatment intranetwork connectivity can predict the outcomes in idiopathic tinnitus patients treated with sound therapy," *Hum. Brain Mapping*, vol. 42, no. 14, pp. 4762–4776, Oct. 2021.

[13] H. Lv et al., "Resting-state functional MRI: Everything that nonexperts have always wanted to know," *Amer. J. Neuroradiol.*, vol. 39, no. 8, pp. 1390–1399, Jan. 2018.

[14] S. M. Smith et al., "Network modelling methods for FMRI," *NeuroImage*, vol. 54, no. 2, pp. 875–891, 2011.

[15] J. Ji, J. Liu, P. Liang, and A. Zhang, "Learning effective connectivity network structure from fMRI data based on artificial immune algorithm," *PLoS ONE*, vol. 11, no. 4, Apr. 2016, Art. no. e0152600.

[16] J. Liu, J. Ji, X. Jia, and A. Zhang, "Learning brain effective connectivity network structure using ant colony optimization combining with voxel activation information," *IEEE J. Biomed. Health Informat.*, vol. 24, no. 7, pp. 2028–2040, Jul. 2020.

[17] J. Liu, J. Ji, G. Xun, and A. Zhang, "Inferring effective connectivity networks from fMRI time series with a temporal entropy-score," *IEEE Trans. Neural Netw. Learn. Syst.*, vol. 33, no. 10, pp. 5993–6006, Oct. 2022.

[18] F. Zeman et al., "Tinnitus handicap inventory for evaluating treatment effects: Which changes are clinically relevant?" *Otolaryngol. Head Neck Surg.*, vol. 145, no. 2, pp. 282–287, Aug. 2011.

[19] J. Wang, X. Wang, M. Xia, X. Liao, A. Evans, and Y. He, "GRETNA: A graph theoretical network analysis toolbox for imaging connectomics," *Frontiers Hum. Neurosci.*, vol. 9, p. 386, Jun. 2015.

[20] L. Fan et al., "The human brainnetome atlas: A new brain atlas based on connectional architecture," *Cerebral Cortex*, vol. 26, no. 8, pp. 3508–3526, 2016.

[21] N. Xu, R. N. Spreng, and P. C. Doerschuk, "Initial validation for the estimation of resting-state fMRI effective connectivity by a generalization of the correlation approach," *Frontiers Neurosci.*, vol. 11, p. 271, May 2017.

[22] S. Shimizu, P. O. Hoyer, A. Hyvärinen, A. Kerminen, and M. Jordan, "A linear non-Gaussian acyclic model for causal discovery," *J. Mach. Learn. Res.*, vol. 7, no. 10, pp. 2003–2030, 2006.

[23] A. K. Seth, "A MATLAB toolbox for Granger causal connectivity analysis," *J. Neurosci. Methods*, vol. 186, no. 2, pp. 262–273, Sep. 2010.

[24] K. J. Friston, A. M. Bastos, A. Oswal, B. van Wijk, C. Richter, and V. Litvak, "Granger causality revisited," *NeuroImage*, vol. 101, pp. 796–808, Nov. 2014.

[25] N. Frolov, V. Maksimenko, A. Lüttjohann, A. Koronovskii, and A. Hramov, "Feed-forward artificial neural network provides data-driven inference of functional connectivity," *Chaos, Interdiscipl. J. Nonlinear Sci.*, vol. 29, no. 9, Sep. 2019, Art. no. 091101.

[26] R. S. Patel, F. D. Bowman, and J. K. Rilling, "A Bayesian approach to determining connectivity of the human brain," *Hum. Brain Mapping*, vol. 27, no. 3, pp. 267–276, 2006.

[27] Q. Chen, H. Lv, Y.-C. Chen, J.-J. Song, and Z. Wang, "Neuroimaging approaches to the study of tinnitus and hyperacusis," *Frontiers Neurosci.*, vol. 15, 2021, Art. no. 700670.

[28] C. M. Krick, H. Argstatter, M. Grapp, P. K. Plinkert, and W. Reith, "Heidelberg neuro-music therapy enhances task-negative activity in tinnitus patients," *Frontiers Neurosci.*, vol. 11, p. 384, Jul. 2017.

[29] L. T. Roland et al., "Effects of mindfulness based stress reduction therapy on subjective bother and neural connectivity in chronic tinnitus," *Otolaryngol., Head Neck Surg.*, vol. 152, no. 5, pp. 919–926, May 2015.

[30] Y.-C. Chen et al., "Tinnitus distress is linked to enhanced resting-state functional connectivity from the limbic system to the auditory cortex," *Hum. Brain Mapping*, vol. 38, no. 5, pp. 2384–2397, May 2017.

[31] G.-P. Zhou et al., "Aberrant functional and effective connectivity of the frontostriatal network in unilateral acute tinnitus patients with hearing loss," *Brain Imag. Behav.*, vol. 16, pp. 151–160, Feb. 2022.

[32] Y. Cai et al., "Aberrant functional and causal connectivity in acute tinnitus with sensorineural hearing loss," *Frontiers Neurosci.*, vol. 14, p. 592, Jun. 2020.

[33] P. A. Stokes and P. L. Purdon, "A study of problems encountered in Granger causality analysis from a neuroscience perspective," *Proc. Nat. Acad. Sci. USA*, vol. 114, no. 34, pp. E7063–E7072, Aug. 2017.

[34] H. Kreft and W. Jetz, "Global patterns and determinants of vascular plant diversity," *Proc. Nat. Acad. Sci. USA*, vol. 104, no. 14, pp. 5925–5930, Apr. 2007.

[35] M.-T. Herrero, C. Barcia, and J. Navarro, "Functional anatomy of thalamus and basal ganglia," *Child's Nervous Syst.*, vol. 18, no. 8, pp. 386–404, Aug. 2002.

[36] J. Zhang, "Auditory cortex stimulation to suppress tinnitus: Mechanisms and strategies," *Hearing Res.*, vol. 295, pp. 38–57, Jan. 2013.

[37] H. Lv et al., "Sound therapy can modulate the functional connectivity of the auditory network," *Prog. Neuro-Psychopharmacol. Biol. Psychiatry*, vol. 110, Aug. 2021, Art. no. 110323.

[38] L. Han et al., "The effects of sound therapy in tinnitus are characterized by altered limbic and auditory networks," *Brain Commun.*, vol. 2, no. 2, Jul. 2020, Art. no. fcaa131.

[39] H. Lv et al., "Altered functional connectivity of the thalamus in tinnitus patients is correlated with symptom alleviation after sound therapy," *Brain Imag. Behav.*, vol. 14, no. 6, pp. 2668–2678, Dec. 2020.

[40] W. Sedley, "Tinnitus: Does gain explain?" *Neuroscience*, vol. 407, pp. 213–228, May 2019.

[41] S. Vanneste, O. Alsalman, and D. De Ridder, "Top-down and bottom-up regulated auditory phantom perception," *J. Neurosci.*, vol. 39, no. 2, pp. 364–378, Jan. 2019.

[42] M.-C. Tsai, Y.-X. Cai, C.-D. Wang, Y.-Q. Zheng, J.-L. Ou, and Y.-H. Chen, "Tinnitus abnormal brain region detection based on dynamic causal modeling and exponential ranking," *BioMed Res. Int.*, vol. 2018, pp. 1–10, Jul. 2018.

[43] W. Singer et al., "Noise-induced inner hair cell ribbon loss disturbs central arc mobilization: A novel molecular paradigm for understanding tinnitus," *Mol. Neurobiol.*, vol. 47, no. 1, pp. 261–279, Feb. 2013.

[44] P. Adjamian, D. A. Hall, A. R. Palmer, T. W. Allan, and D. R. M. Langers, "Neuroanatomical abnormalities in chronic tinnitus in the human brain," *Neurosci. Biobehav. Rev.*, vol. 45, pp. 119–133, Sep. 2014.

[45] S. E. Shore, L. E. Roberts, and B. Langguth, "Maladaptive plasticity in tinnitus—Triggers, mechanisms and treatment," *Nature Rev. Neurol.*, vol. 12, no. 3, pp. 150–160, Mar. 2016.

[46] D. De Ridder, S. Vanneste, B. Langguth, and R. Llinas, "Thalamocortical dysrhythmia: A theoretical update in tinnitus," *Frontiers Neurol.*, vol. 6, p. 124, Jun. 2015.

[47] P. A. Tass, I. Adamchic, H.-J. Freund, T. von Stackelberg, and C. Hauptmann, "Counteracting tinnitus by acoustic coordinated reset neuromodulation," *Restorative Neurol. Neurosci.*, vol. 30, no. 2, pp. 137–159, 2012.

[48] X. Wang, Y. Tan, O. Van den Bergh, A. von Leupoldt, and J. Qiu, "Intrinsic functional brain connectivity patterns underlying enhanced interoceptive sensibility," *J. Affect. Disorders*, vol. 276, pp. 804–814, Nov. 2020.

[49] M. S. Beauchamp, "See me, hear me, touch me: Multisensory integration in lateral occipital-temporal cortex," *Current Opinion Neurobiol.*, vol. 15, no. 2, pp. 145–153, Apr. 2005.